Validation and application of optimal ionospheric shell height model for single-site TEC estimation

Jiaqi Zhao[1], Chen Zhou[1]

School of Electronic Information, Wuhan University, Wuhan, 430072, China

Corresponding to: chenzhou@whu.edu.cn

Abstract

We recently proposed a method to establish an optimal ionospheric shell height model based on the international GNSS service (IGS) station data and the differential code bias (DCB) provided by Center for Orbit Determination in Europe (CODE) during the time from 2003 to 2013. This method is very promising for DCB and accurate total electron content (TEC) estimation by comparing to the traditional fixed shell height method. However, this method is basically feasible only for IGS stations. In this study, we investigate how to apply the optimal ionospheric shell height derived from IGS station to non-IGS stations or isolated GNSS receivers. The intuitive and practical method to estimate TEC of non-IGS stations is based on optimal ionospheric shell height derived from nearby IGS stations. To validate this method, we selected two dense networks of IGS stations located in regions in US and Europe. Two optimal ionospheric shell height models are established by two reference stations, namely GOLD and PTBB, which are located at the approximate center of two selected regions. The predicted daily optimal ionospheric shell heights by the two models are applied to other IGS stations around these two reference stations. Daily DCBs are calculated according to these two optimal shell heights and compared to respective DCBs released by CODE. The validation results of this method present that 1) Optimal ionospheric shell height calculated by IGS stations can be applied to its nearby non-IGS stations or isolated GNSS receivers for accurate TEC estimation. 2) As the distance away from the reference IGS station becomes larger, the DCB estimation error becomes larger. The relation between the DCB estimation error and the distance is generally linear.

Keyword

Ionospheric shell height, Single layer model (SLM), Differential code bias (DCB), Total electron content (TEC)

Introduction

Dual-frequency GPS signal propagation is affected effectively by ionospheric dispersive characteristics. Taking advantage of this property, ionospheric TEC along the path of signal can be estimated by differencing the pseudorange or carrier phase observations from dual-frequency GPS signals. Carrier phase leveling/smoothing of code measurement is widely adopted to improve the precision of absolute TEC observations (Mannucci et al., 1998; Horvath and Crozier, 2007). In general, it is considered that the derived TEC in carrier phase leveling/smoothing technique consists of slant TEC (STEC), the combination differential code bias (DCB) of satellite and receiver, multipath effects and noise. The DCB is usually considered as the main error source and could be as large as several TECu (Lanyi and Roth, 1988; Warnant 1997).

For TEC and DCB estimations, mapping functions with a single layer model (SLM) assumption have been intensively studied for many years. Sovers and Fanselow (1987) firstly simplified the ionosphere to a spherical shell. They set the bottom and the top side of the ionospheric shell as h-35 and h+75 km, where h is taken to be 350 km above the surface of the earth and allowed to be adjusted. In this model, the electron density was evenly distributed in the vertical direction. Based on this model, Sardón et al. (1994) introduced the Kalman filter method for real-time ionospheric VTEC estimation, which can also be a promising prediction of DCBs under adverse conditions (antispoofing, ionospheric disturbances). Klobuchar (1987) assumed that STEC equals VTEC multiplied by the approximation of the standard geometric mapping function at the mean vertical height of 350 km along the path of STEC. Lanyi and Roth (1988) further developed this model into a single thin-layer model, and proposed the standard geometric mapping function and the polynomial model. The single thin-layer model assumed that the ionosphere is simplified by a spherical thin shell with infinitesimal thickness. Clynch et al (1989) proposed a mapping function in the form of a polynomial by assuming a homogeneous electron density shell between altitudes of 200 and 600 km. Mannucci et al (1998) presented an elevation scaling mapping function derived from the extended slab mode. There are also many modified mapping functions according to the standard geometric mapping function. Schaer (1999) proposed the modified standard mapping function using a reduced zenith angle. Rideout and Coster (2006) presented a new mapping function which replaces the influence of the shell height by an adjustment parameter, and set the shell height as 450 km. Smith et al (2008) modified the standard mapping function by using a complex factor. Based on the electron density field derived from the international reference ionosphere (IRI), Zus et al (2017) recently developed an ionospheric mapping function at fixed height of 450 km with dependence on time, location, azimuth angle, elevation angle, and different frequencies.

The ionospheric shell height is considered to be the most important parameter for a mapping function, and the shell height is typically set to a fixed value between 350 and 450 km (Lanyi and Roth, 1988; Mannucci et al., 1998). Birch et al. (2002) proposed an inverse method to estimate the shell height by using simultaneous VTEC and STEC observations, and suggested the shell height is preferred to be a value between 600 and 1200 km. Nava et al. (2007) utilized multiple stations to obtain a shell height estimation method by minimizing the mapping function errors, this method is referred as the “coinciding pierce point” technique. Their results indicated that the suitable shell heights for the mid-latitude is 400 km and 500 km during the geomagnetic undisturbed conditions and disturbed conditions, respectively. In the case of the low-latitude, the shell height at about 400 km is suitable for both quiet and disturbed geomagnetic conditions. Jiang et al. (2018) applied this technique to estimate the optimal shell height for different latitude bands. In their case, the optimal layer height is about 350 km for the entire globe. Brunini et al. (2011) studied the influence of the shell height by using an empirical model of the ionosphere, and pointed out that a unique shell height for whole region does not exist. Li et al. (2018) applied a new determination method of the shell height based on the combined IGS GIMs and the two methods mentioned above to the Chinese region, and indicated that the optimal shell height in China ranges from 450 to 550 km. Wang et al. (2016) studied the shell height for a grid-based algorithm by analyzing goodness of fit for STEC. Lu et al. (2017) applied this method to different VTEC models, and investigated the optimal shell heights at solar maximum and at solar minimum.

In the recent study by Zhao and Zhou (2018), a method to establish an optimal ionospheric shell height model for single station VTEC estimation has been proposed. This method calculates the optimal ionospheric shell height with regards to minimize |ΔDCB| by comparing to the DCB released by CODE. Five optimal ionospheric shell height models were established by the proposed method based on the data of five IGS stations at different latitudes and the corresponding DCBs provided by CODE during the time 2003 to 2013. For the five selected IGS stations, the results have shown that the optimal ionospheric shell height models improve the accuracies of DCB and TEC estimation compared to a fixed ionospheric shell height of 400 km in a statistical sense. We also found that the optimal ionospheric shell height shows 11-year and 1-year periods and is correlated to the solar activity, which indicated the connection of the optimal shell height with ionospheric physics.

While the proposed optimal ionospheric shell height model is promising for DCB and TEC estimation, this method also can be implemented to isolated GNSS receivers not belonging to IGS stations, if we can get the long-term observations and reference values of DCB from the isolated GNSS receivers. By considering the spatial correlation of ionospheric electron density, it is intuitive and practical to adopt the optimal ionospheric shell height of a nearby IGS station to the non-IGS stations. So whether an optimal ionospheric shell height model can improve the TEC/DCB estimation of nearby stations needs to be verify.

The purpose of this study is to investigate the feasibility of applying the optimal ionospheric shell height model derived from IGS station to nearby non-IGS GNSS receivers for accurate TEC/DCB estimation. By selecting two different regions in U.S. and Europe with dense IGS stations, we calculate the daily DCBs of 2014 by using the optimal ionospheric shell heights derived from data from 2003-2013 of two central stations in two regions. We also try to find the DCB estimation error and its relation to the distance away from the central reference station.

Method

In (Zhao and Zhou, 2018), we proposed a concept of optimal ionospheric shell height for accurate TEC and DCB estimation. Based on daily data of a single site, this approach searches a daily optimal ionospheric shell height, which minimizes the difference between the DCBs calculated by the VTEC model for a single site and reference values of DCB. For a single site, its long-term daily optimal ionospheric shell heights can be estimated and then modeled. In our case, the polynomial model (Wild, 1994; Komjathy, 1997) is applied to estimate satellite and receiver DCBs, and the DCBs provided by CODE are used as the reference.

In the polynomial model, the VTEC is considered as a Taylor series expansion in latitude and solar hour angle, which is expressed as follows:

$$T_V(\varphi, S) = \sum_{i=0}^{m}\sum_{j=0}^{n} E_{ij}(\varphi - \varphi_0)^i (S - S_0)^j \tag{1}$$

where T_V denotes VTEC. φ and S denote the geographic latitude and the solar hour angle of ionospheric pierce point (IPP), respectively; φ_0 and S_0 denote φ and S at the center of the cover region of IPP in one day. E_{ij} is the model coefficient. m and n denote the orders of the model. A polynomial model fits the VTEC over a period of time. In our case, a VTEC model is generated over 3 hours of time, therefore 8 VTEC models are applied per day. DCB is considered as constant in one day. Since our analysis is based on long-term single site data, we set *m* and *n* to 4 and 3, respectively. Huang and Yuan (2014) applied the polynomial model with the same orders to TEC estimation.

Based on the thin shell approximation, the observation equation can be written as:

$$T_{os}^{PRN}(\varphi, S) = T_V(\varphi, S) \cdot f(z) + DCB^{PRN} \tag{2}$$

where T_{os}^{PRN} is slant TEC calculated by carrier phase smoothing, the superscript *PRN* denotes GPS satellite. DCB^{PRN} denotes the combination of GPS satellite and receiver DCB. z denotes the zenith angle of IPP. According to Lanyi and Roth (1988), the standard geometric mapping function $f(z)$ is expressed as follows:

$$f(z) = 1/\cos(z) \tag{3}$$

$$z = \arcsin \frac{\mathrm{Re} \cdot \cos El}{\mathrm{Re} + h} \tag{4}$$

where Re denotes the earth's radius, El denotes the elevation angle, and h denotes the thin ionospheric shell height. Note that h also affects the location of the IPP.

To estimate DCBs, the method above requires a definite thin shell height value. Conversely, if we get the daily solutions of DCBs, the optimal ionospheric shell height can be estimated. The optimal ionospheric shell height is assumed to be between 100 and 1000 km and is defined as the shell height with the minimum difference between DCB^{PRN} and the reference values. This optimization problem can be written as:

$$\min_{100<h<1000} mean\left(\left|\mathbf{DCB_{ref}} - \mathbf{DCB}\right|\right) \text{ s.t. } \mathbf{T} = \mathbf{\Phi} \cdot \mathbf{E} + \boldsymbol{\theta} \cdot \mathbf{DCB} \tag{5}$$

where h is the daily optimal ionospheric shell height; $\mathbf{DCB_{ref}}$ denotes the vector of the reference values of DCBs; s.t. is the abbreviation for subject to; $\mathbf{T} = \mathbf{\Phi} \cdot \mathbf{E} + \boldsymbol{\theta} \cdot \mathbf{DCB}$ is the matrix form of all the observation equations in one day; $\mathbf{T}$ denotes the vector of T_{os}; $\mathbf{E}$ corresponds to the coefficients of the models, contains E_{ij}; $\mathbf{DCB}$ is the vector of DCB^{PRN}; $\mathbf{\Phi}$ is the coefficient matrix of $\mathbf{E}$, contains $(\varphi - \varphi_0)^i (S - S_0)^j f(z)$; and $\boldsymbol{\theta}$ is the coefficient matrix of $\mathbf{DCB}$, contains only 1s and 0s. **E** and **DCB** are unknown.

After the method above is applied to 11-year data, the estimated optimal ionospheric shell heights can be modeled by a Fourier series, which is expressed as follows:

$$h(x) = a_0 + \sum_{n=1}^{k}\left(a_n \cos\frac{2n\pi x}{L} + b_n \sin\frac{2n\pi x}{L}\right) \tag{6}$$

where k is the order of Fourier series and is set to 40, a_n and b_n are the model coefficients, x is the time, and L is the time span which equals to 4018 days. The maximum frequency of the model is 40/L≈0.01 per day, which corresponds to a period of 100 days. By least square method, the model coefficients can be estimated.

This model can be applied to neighboring stations' DCB estimation. Instead of fixed shell height, this model provides a predicted optimal ionospheric shell height. Note that, while in the establishment and application of the model, the VTEC model, mapping function and elevation cut-off angle are constant, all of them affect the optimal ionospheric shell height.

Experiment and Results

The previous section introduced a method to establish a daily optimal ionospheric shell height model based on a single site with reference values of DCBs. To analyze the improvement of DCB estimation by this model for the reference station and other neighboring stations, we present two experiments to evaluate and validate this method by using IGS stations located in region in U.S. and Europe. To ensure the accuracy and consistency of DCB, we only select IGS stations with pseudorange measurements of P1 code, and whose receiver DCBs have been published by CODE.

Figure 1 presents the location and distribution of the selected IGS stations in two regions. Table 1 presents the information of the geographical location, distance to reference station in each region and receiver types of all stations. Based on the RINEX data of the GOLD station in Region I and the PTBB station in Region II during the period of 2003-2013, two separate optimal ionospheric shell height models for each region are established by the aforementioned method. Then the model is applied to estimate DCB in 2014 for all the other stations in each region. Note that the reference stations GOLD and PTBB are marked with black triangles in the figure. The other neighboring stations are located in different orientations of GOLD and PTBB with different distances, which range from 136 to 1159 km for region I and range from 190 to 1712 km for region II. In the table, the receiver type is corresponding to 2003~2014 for GOLD and PTBB, and 2014 for the other stations. In region I, the receiver type of GOLD has been changed once in September 2011. The five selected stations used four receiver types in 2014; TABV and PIE1 had the same receiver type. In region II, there are nine receiver types for the sixteen stations. The receiver type of PTBB has changed twice in 2006.

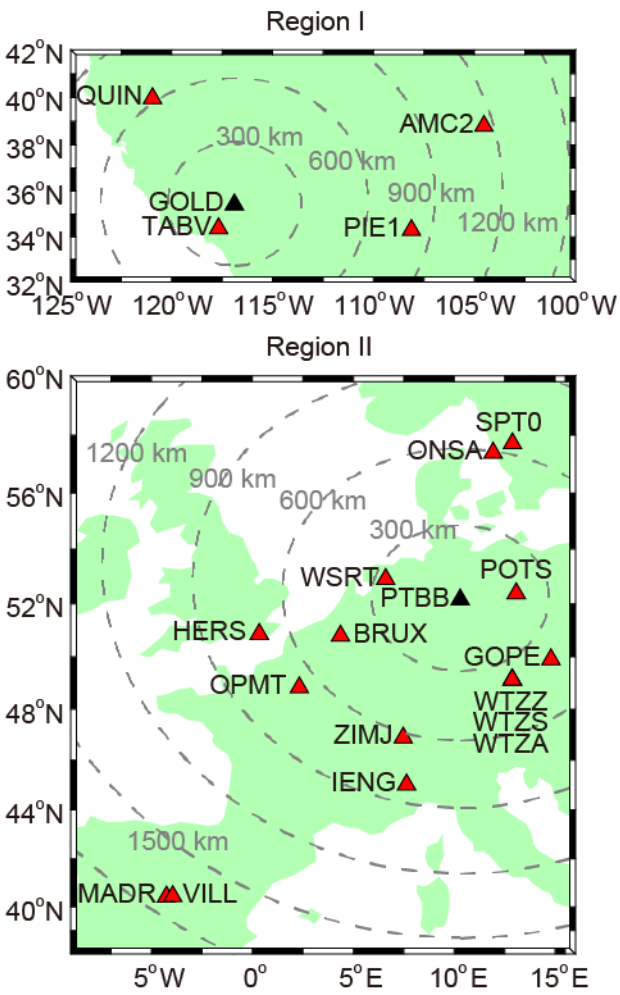

Fig.1 Geographical location of the selected IGS stations in U.S. region (Region I) and Europe region (Region II). The black triangle in each plot is the reference station.

Table 1 Information for the stations

Name	Latitude (deg)	Longitude (deg)	Distance to GOLD or PTBB (km)	Receiver type and service date
GOLD	35.42	-116.89	0	ASHTECH Z-XII3 ~ 2011-09-14 JPS EGGDT 2011-09-19 ~
TABV	34.38	-117.68	136.67	JAVAD TRE_G3TH DELTA

QUIN	39.97	-120.94	619.55	ASHTECH UZ-12
PIE1	34.30	-108.12	810.51	JAVAD TRE_G3TH DELTA
AMC2	38.80	-104.52	1159.09	ASHTECH Z-XII3T
PTBB	52.15	10.30	0	SEPT POLARX2 2006-07-25~2006-11-13 ASHTECH Z-XII3T else
POTS	52.38	13.07	190.82	JAVAD TRE_G3TH DELTA
WSRT	52.91	6.60	264.92	AOA SNR-12 ACT
WTZA	49.14	12.88	381.28	ASHTECH Z-XII3T
WTZS	49.14	12.88	381.28	SEPT POLARX2
WTZZ	49.14	12.88	381.28	JAVAD TRE_G3TH DELTA
GOPE	49.91	14.79	401.51	TPS NETG3
BRUX	50.80	4.36	439.03	SEPT POLARX4TR
ONSA	57.40	11.93	593.72	JPS E_GGD
ZIMJ	46.88	7.47	620.79	JAVAD TRE_G3TH DELTA
SPT0	57.72	12.89	641.78	JAVAD TRE_G3TH DELTA
OPMT	48.84	2.33	674.24	ASHTECH Z-XII3T
HERS	50.87	0.34	705.38	SEPT POLARX3ETR
IENG	45.02	7.64	816.64	ASHTECH Z-XII3T
VILL	40.44	-3.95	1696.62	SEPT POLARX4
MADR	40.43	-4.25	1712.27	JAVAD TRE_G3TH DELTA

Figure 2 presents the estimated daily optimal ionospheric shell height of GOLD and PTBB during the period from 2003 to 2013. The left panel shows the variation of the daily optimal ionospheric shell height and the fitting result by (6). From the overall trend, the variations of daily optimal ionospheric shell height for both two stations appear wave-like oscillations during the 11 years period. In the right panel, the statistical result are fitted by a normal distribution. The mean and the standard deviation (STD) of the normal distribution are 714.3 and 185.4 km for GOLD, respectively. The mean and STD value for PTBB is 416.4 and 184.1 km, respectively. At the end of 2010, a gap appears, for the DCB provided by CODE is simultaneously anomalous for both stations (Zhao and Zhou, 2018), and the data during this period are abandoned.

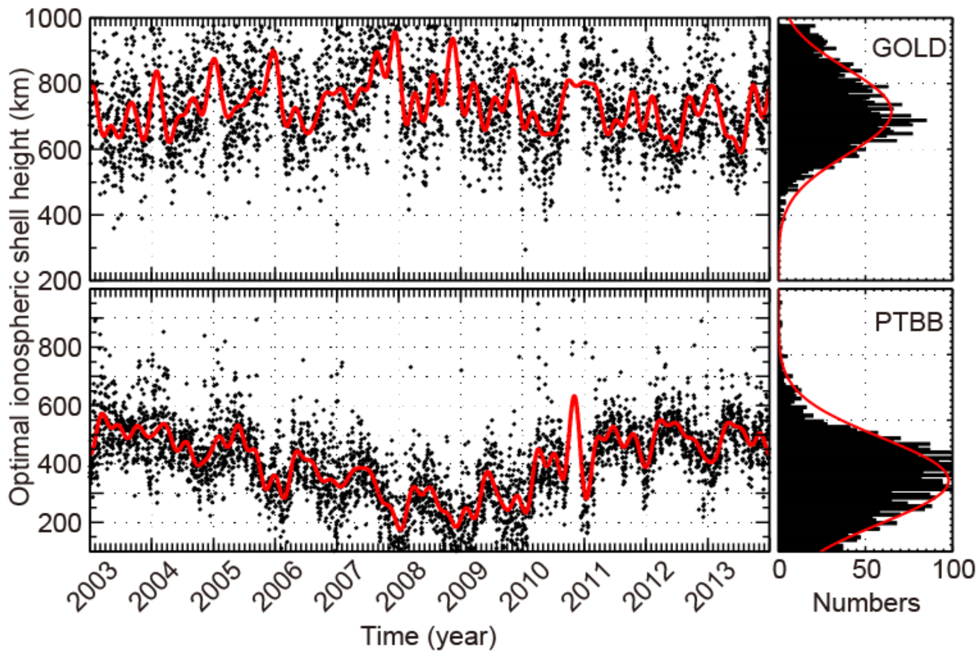

Fig.2 Variation of the daily optimal ionospheric shell height (black) and the fitting result (red)

Figure 3 presents the amplitude spectra of the daily optimal ionospheric shell height of the two reference stations estimated by the Lomb-Scargle analysis (Lomb, 1976; Scargle, 1982). As can be found in Figure 3, the peaks correspond to 11-year, 1-year, 6-month and 4-month cycles. The amplitudes of 11-year and 1-year cycles are more evident than other periods in both two stations. As mentioned earlier, 0.01 per day is about the maximum frequency of (6). Higher frequencies would not be useful because of their small amplitudes. This result shows that the optimal ionospheric shell height of GOLD and PTBB is periodic, and the 40th-order of Fourier series is suitable for modelling its variation.

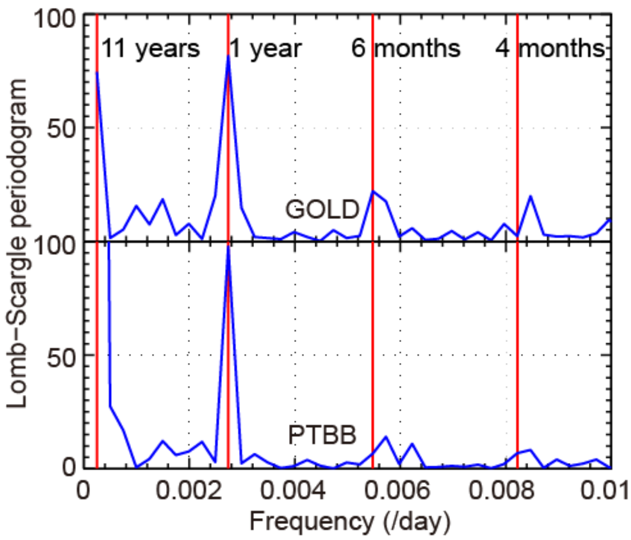

Fig.3 Lomb-Scargle spectra of the daily optimal ionospheric shell height

We establish two optimal ionospheric shell height models for each region from the 40th-order Fourier series based on the 11-year data of GOLD and PTBB. To investigate the availability zone of the optimal ionospheric shell height model, we apply the models to the stations of each region as shown in Figure 1 and Table 1. Based on the predicted daily optimal ionospheric shell heights in 2014 calculated by the model at GOLD or PTBB, each station is applied to estimate DCB separately in 2014 using equation (1)-(4). The difference of DCBs in all stations in each region calculated using the optimal ionospheric shell height model at the reference stations and DCBs provided by CODE is then compared to the difference of DCBs calculated using a fixed ionospheric shell height (400 km) and DCBs released by CODE.

The results of this comparison are shown in Figure 4. The panels for the stations are arranged by their distances to reference station, this is also applied to Table 2; from the top panels to the bottom panels, the distance of the corresponding station to the reference station gradually increases. The left and right panels show the daily differences and the histograms of the statistical results in 2014, respectively. For all of the stations, the daily average differences of DCBs calculated using the optimal ionospheric shell height model are reduced compared to those using the fixed ionospheric shell height. For GOLD and TABV, the improvement is substantial, the daily average ΔDCBs is close to zero. For the other stations, the median daily average ΔDCB is negative, but smaller in absolute value than using the fixed shell height. This result shows the improvement of the model seems to be related with the distance to GOLD. Data gaps on the figure correspond to days when data from that station are not available. Figure 5 is the same format as Figure 4, and presents the results of Region II. Comparing to the results of fixed ionospheric height, Figure 5 also indicates that the ΔDCB calculated using the optimal ionospheric shell heights at PTBB is on average smaller than that calculated using fixed ionospheric shell height. Both Figure

4 and Figure 5 present that the accuracy of DCB estimation can be improved using optimal ionospheric heights from reference stations.

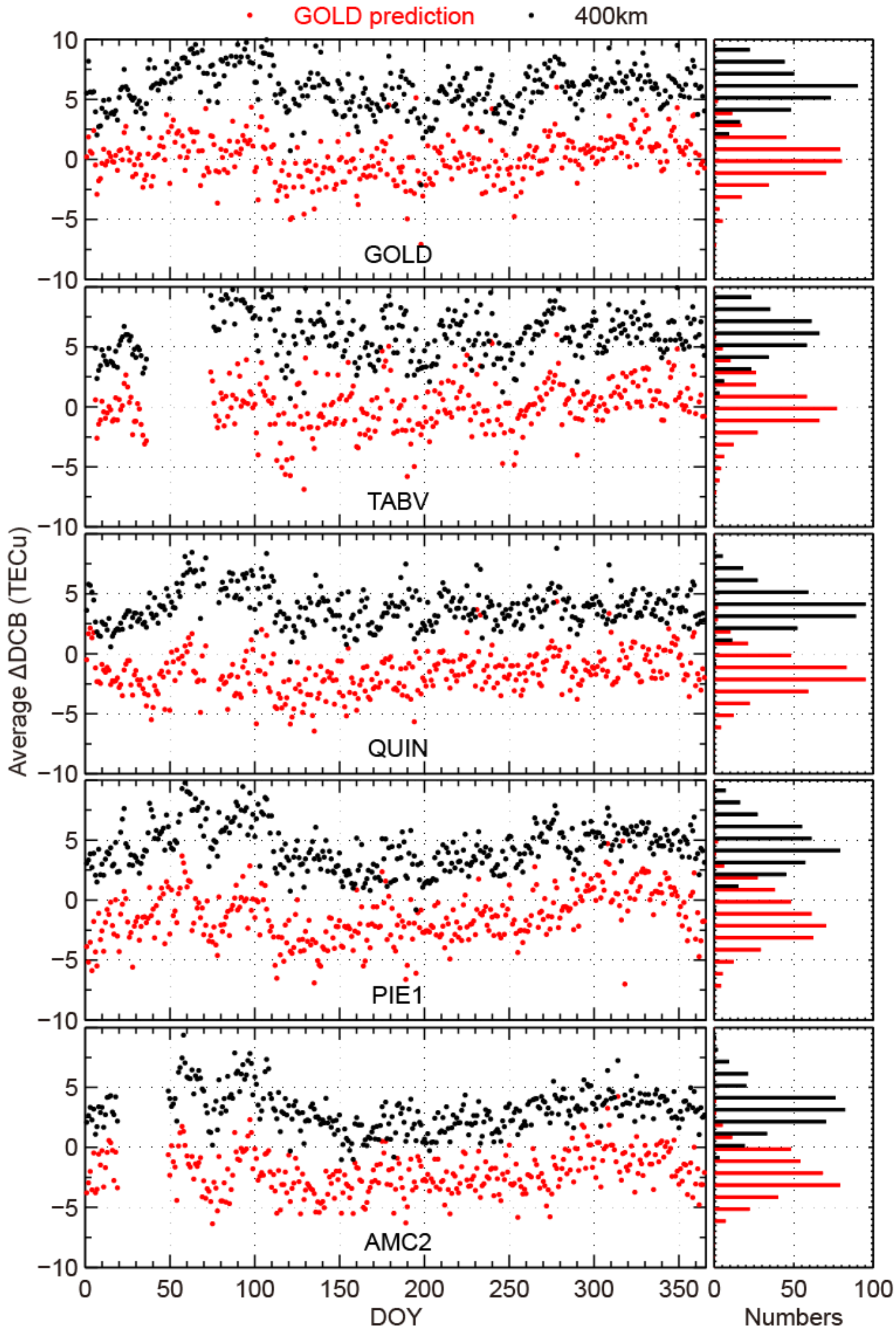

Fig.4 Comparisons of the average ΔDCB calculated using the predicted optimal

ionospheric shell heights (red dots) and those using the fixed ionospheric shell height (black dots) in 2014 for stations in Region I.

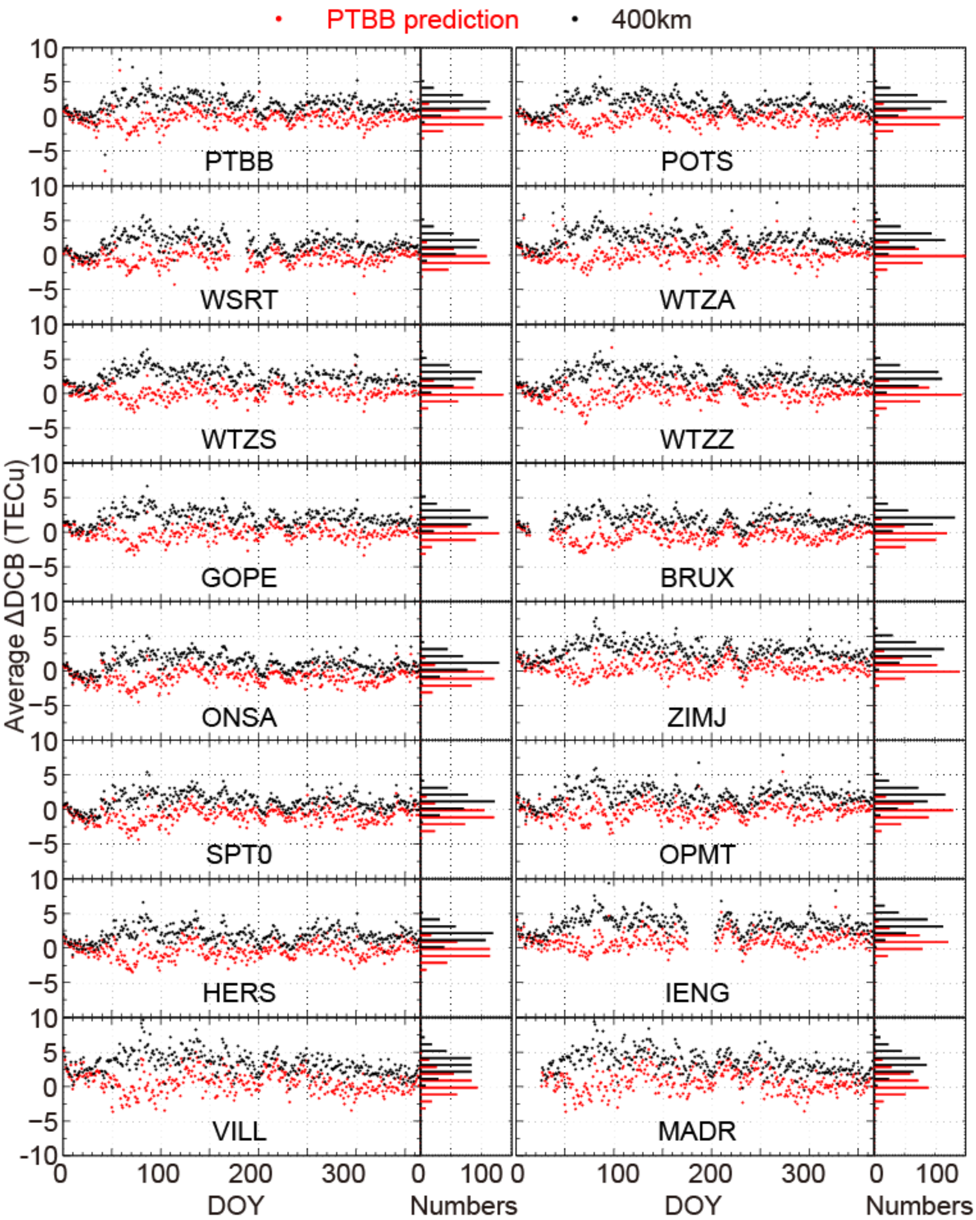

Fig.5 Comparisons of the average ΔDCB calculated using the predicted optimal ionospheric shell heights (red dots) and those using the fixed ionospheric shell height

(black dots) in 2014 for stations in Region II.

Table 2 presents the quantitative statistical results of average ΔDCB in 2014. For all the stations in each region, the mean values and the root mean squares (RMS) using the optimal ionospheric shell height model are smaller than those using the fixed ionospheric height. For Region I, the improvements of GOLD and TABV are the most significant. Their mean values are reduced to 0.12 and 0.08 TECu, respectively; the root mean squares are reduced by 4.43 and 4.33 TECu, respectively. For Region II, the improvement for DCB estimation are the most obvious for WTZZ, with mean value of ΔDCB decreases from 2.34 to 0.02. We could note that TABV and WTZZ station are quite close to the reference stations in each region.

Table 2 Statistical results of mean (ΔDCB) in 2014

Station	Average ΔDCB (TECu) Optimal Ionospheric Height		Average ΔDCB (TECu) Fixed Ionospheric Height	
	Mean	RMS	Mean	RMS
GOLD	0.12	1.82	5.96	6.25
TABV	0.08	2.04	6.06	6.37
QUIN	-1.60	2.31	3.91	4.19
PIE1	-1.38	2.50	4.46	4.84
AMC2	-2.12	2.75	3.09	3.53
PTBB	-0.28	1.23	1.82	2.26
POTS	-0.27	1.00	1.84	2.18

WSRT	-0.41	1.14	1.65	2.10
WTZA	0.09	1.20	2.38	2.73
WTZS	0.14	0.99	2.48	2.76
WTZZ	0.02	1.14	2.34	2.65
GOPE	-0.17	1.00	2.12	2.41
BRUX	-0.42	1.12	1.86	2.13
ONSA	-0.88	1.40	1.10	1.63
ZIMJ	0.48	1.17	2.87	3.13
SPT0	-0.84	1.40	1.14	1.67
OPMT	-0.29	1.21	1.93	2.35
HERS	-0.37	1.19	1.84	2.19
IENG	1.05	1.57	3.44	3.69
VILL	0.59	1.67	3.30	3.66
MADR	0.66	1.71	3.50	3.86

Figure 6 and Figure 7 present the relation between the statistical results of average ΔDCB and the distance to the reference stations in each region. The left and the right panels in each figure show the relation of the absolute mean value and the root mean square, respectively. with the distance to GOLD or PTBB. For all of the stations, the optimal ionospheric shell height model improves the accuracies of DCB estimation compared to the fixed ionospheric shell height in a statistical sense; both of the absolute mean values and the root mean squares become smaller. For the optimal ionospheric shell height model, the absolute mean values show a positive correlation with the distance to reference station GOLD or PTBB in each region, as well as the root mean squares. By using the linear regression, for Region I, the absolute mean value increases at a rate of about 1.84 TECu per 1000 km and starts at about 0.05 TECu. The RMS value increases at a rate of about 0.75 TECu per 1000 km and starts at about 1.87 TECu. According to the fitting results, the absolute mean value and the RMS are less than 1 TECu and 2.25 TECu in the region around GOLD with a radius of 500 km, and less than 2 TECu and 2.62 TECu for the region with a radius of 1000 km. For Region II, the absolute mean value increases at a rate of about 0.30 TECu per 1000 km and start at about 0.25 TECu. The RMS value increases at a rate of about 0.41 TECu per 1000 km and starts at about 1.01 TECu. According to the fitting results, the absolute mean value and the RMS less than about 0.40 TECu and 1.21 TECu in the region around PTBB with a radius of 500 km, and less than about 0.55 TECu and 1.42 TECu for the region with a radius of 1000 km. For the two regions, the RMSs present stronger linear relations with distance than the means.

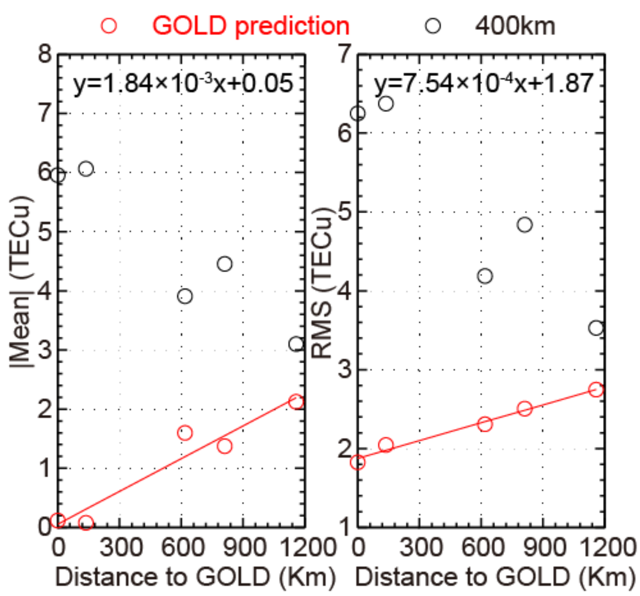

Fig.6 Relation of the accuracy for DCB estimation with the distance to GOLD. The red lines are the linear fitting results

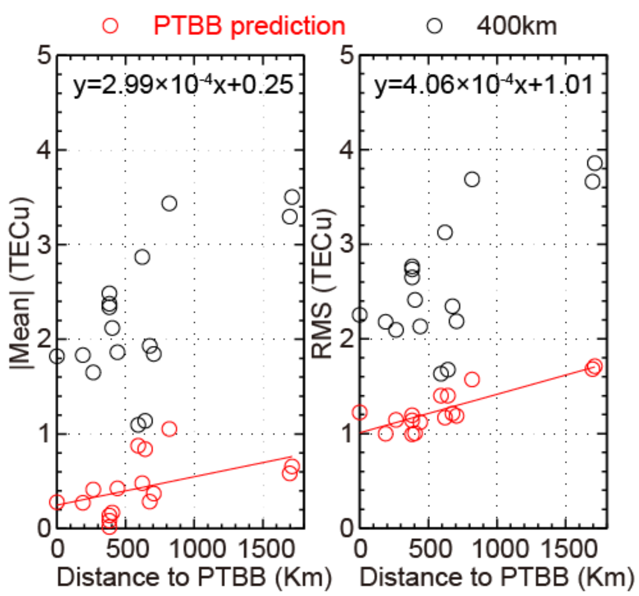

Fig.7 Relation of the accuracy for DCB estimation with the distance to PTBB. The red lines are the linear fitting results

Summary

In this study, we implement and validate a method to transfer the optimal ionospheric shell height derived for IGS stations to non-IGS stations or isolated GNSS receivers. We establish two optimal ionospheric shell height models by the 40th-order Fourier series based on the data of IGS stations GOLD and PTBB in two separate regions These two models are applied to the stations in each region, where the distance to

GOLD ranges from 136 to 1159 km and the distance to PTBB ranges from 190. to 1712 km. The main findings are summarized as follows:

1) The optimal ionospheric shell height model improves the accuracy of DCB estimation comparing to the fixed shell height for all of the stations in a statistical sense. These results indicate the feasibility of applying the optimal ionospheric shell height derived from IGS station to other neighboring stations. The IGS stations can calculate and predict the daily optimal ionospheric shell height, and then release this value to the nearby non-IGS stations or isolated GNSS receivers.

2) For other stations in each region, the error of DCB by the optimal ionospheric shell height increases linearly with the distance to the reference station GOLD or PTBB. For the mean and the RMS of the daily average ΔDCBs, in region I, the slopes are about 1.84 and 0.75 TECu per 1000 km; in region II, the slopes are about 0.30 and 0.41 TECu per 1000 km. These results indicate the horizontal spatial correlation of regional ionospheric electron density distribution. For the different region, the error at 0 km (i.e. the error for the reference station) is different, which should be also considered, the quality of the DCB estimations also depends on the quality of the optimal shell height model at the reference stations themselves.

Due to a requirement of this experiment, we only analyze two regions in mid-latitude because of the insufficiency of long-term P1 data. We also ignore the orientation of isolated GPS receivers to the reference station.

Acknowledgments

This study is based on data services provided by the IGS (International GNSS Service) and CODE (the Center for Orbit Determination in Europe). This work is supported by the National Natural Science Foundation of China (NSFC grant 41574146 and 41774162).

Reference

Birch, M. J., Hargreaves, J. K., Bailey, G. J.: On the use of an effective ionospheric height in electron content measurement by GPS reception, Radio Sci., 37, 1015, doi: 10.1029/2000RS002601, 2002.

Brunini, C., Camilion, E., Azpilicueta, F.: Simulation study of the influence of the ionospheric layer height in the thin layer ionospheric model, J. Geod., 85, 637–645, doi: 10.1007/s00190-011-0470-2, 2011.

Clynch, J. R., Coco, D. S., Coker, C. E.: A versatile GPS ionospheric monitor: high latitude measurements of TEC and scintillation, in: Proceedings of ION GPS-89, the 2nd International Technical Meeting of the Satellite Division of The Institute of Navigation, Colorado Springs, CO, 22–27 September 1989, 445-450, 1989.

Horvath, I., Crozier, S.: Software developed for obtaining GPS-derived total electron content values, Radio Sci., 42, RS2002, doi: 10.1029/2006RS003452, 2007.

Huang, Z., Yuan, H.: Ionospheric single-station TEC short-term forecast using RBF neural network, Radio Sci., 49, 283–292, doi: 10.1002/2013RS005247, 2014.

Jiang, H., Wang, Z., An, J., Liu, J., Wang, N., Li, H.: Influence of spatial gradients on ionospheric mapping using thin layer models, GPS Solut., 22, 2, doi: 10.1007/s10291-017-0671-0, 2018.

Klobuchar, A.: Ionospheric time-delay algorithm for single-frequency GPS users, IEEE Trans. Aerosp. Electron. Syst., AES-23, 325–331, 1987.

Komjathy, A.: Global Ionospheric Total Electron Content Mapping Using the Global Positioning System, Ph.D. thesis, Department of Geodesy and Geomatics Engineering Technical Report NO. 188, University of New Brunswick, Fredericton, New Brunswick, Canada, 248 pp., 1997.

Lanyi, G. E., Roth, T.: A comparison of mapped and measured total ionospheric electron content using Global Positioning System and beacon satellite observations, Radio Sci., 23, 483–492, doi: 10.1029/RS023i004p00483, 1988.

Li, M., Yuan, Y., Zhang, B., Wang, N., Li, Z., Liu, X., Zhang, X.: Determination of the optimized single-layer ionospheric height for electron content measurements over China, Journal of Geodesy, 92, 169-183, doi: 10.1007/s00190-017-1054-6, 2018.

Lomb, N. R.: Least-squares frequency analysis of unequally spaced data, Astrophysics and space science, 39, 447-462, doi: 10.1007/BF00648343, 1976.

Lu, W., Ma, G., Wang, X., Wan, Q., Li, J.: Evaluation of ionospheric height assumption for single station GPS-TEC derivation, Advances in Space Research, 60, 286-294, doi: 10.1016/j.asr.2017.01.019, 2017.

Mannucci, A. J., Wilson, B. D., Yuan, D. N., Ho, C. H., Lindqwister, U. J., Runge, T. F.: A global mapping technique for GPS-derived ionospheric total electron content measurements, Radio Sci. 33, 565–583, doi: 10.1029/97RS02707, 1998.

Nava, B., Radicella, S. M., Leitinger, R., Coïsson, P.: Use of total electron content data to analyze ionosphere electron density gradients, Adv. Space Res., 39, 1292–1297, doi: 10.1016/j.asr.2007.01.041, 2007.

Rideout, W., Coster, A.: Automated GPS processing for global total electron content data, GPS Solut., 10, 219–228, doi: 10.1007/S10291-006-0029-5, 2006.

Sardón, E., Rius, A., Zarraoa, N.: Estimation of the transmitter and receiver differential biases and the ionospheric total electron content from global positioning system observations, Radio Science, 29, 577–586, doi: 10.1029/94RS00449, 1994.

Scargle, J. D.: Studies in astronomical time series analysis. II-Statistical aspects of spectral analysis of unevenly spaced data, The Astrophysical Journal, 263, 835-853, doi: 10.1086/160554, 1982.

Schaer, S.: Mapping and predicting the earth's ionosphere using the global positioning system, Ph.D. thesis, Astronomical Institute, University of Bern, Bern, Switzerland, 196 pp., 1999.

Smith, D. A., Araujo-Pradere, E. A., Minter, C., Fuller-Rowell, T.: A comprehensive evaluation of the errors inherent in the use of a two-dimensional shell for modeling the ionosphere, Radio Sci., 43, RS6008, doi: 10.1029/2007RS003769, 2008.

Sovers, O. J., Fanselow, J. L.: Observation model and parameter partials for the JPL VLBI parameter estimation software MASTERFIT-1987, JPL Publication, California, , 68 pp, 1987.

Wang, X. L., Wan, Q. T., Ma, G. Y., Li, J. H., Fan, J. T.: The influence of ionospheric thin shell height on TEC retrieval from GPS observation, Res. Astron. Astrophys., 16, 116, doi: 10.1088/1674-4527/16/7/116, 2016.

Warnant, R.: Reliability of the TEC computed using GPS measurements—the problem of hardware biases, Acta Geodaetica et Geophysica Hungarica, 32, 451–459, doi: 10.1007/BF03325514, 1997.

Wild, U.: Ionosphere and satellite systems: permanent GPS tracking data for modelling and monitoring, Ph.D. thesis, Astronomical Institute, University of Bern, Bern, Switzerland, 155 pp., 1994.

Zhao, J., Zhou, C.: On the Optimal Height of Ionospheric Shell for Single-Site TEC Estimation, GPS Solut., 22, 48, doi: 10.1007/s10291-018-0715-0, 2018.

Zus, F., Deng, Z., Heise, S., Wickert, J.: Ionospheric mapping functions based on electron density fields, GPS Solut., 21, 873-885, doi: 10.1007/s10291-016-0574-5, 2017.